UNIVERSITY OF CALIFORNIA, SAN DIEGO

Designer Self Assembly: Distance, Coordination, and Orientation Control of Plasmonic Nanoparticles

A Thesis submitted in partial satisfaction of the requirements
for the degree Master of Science

in

Nanoengineering

by

Yahya Mustafa Alvi

Committee in charge:

Professor Andrea Tao
Professor Darren Lipomi
Professor Donald Sirbuly

2014

The Thesis of Yahya Mustafa Alvi is approved and it is acceptable in quality and form for publication on microfilm and electronically:

Chair

University of California, San Diego

2014

DEDICATION

Dedicated to my loving parents Rukhshanda Alvi and Mohiuddin Alvi, as well as my beautiful sisters Khadija Alvi-Khalid, Soha Alvi, Zoha Alvi

EPIGRAPH

“Impossible is just a big word thrown around by small men who find it easier to live in the world they've been given than to explore the power they have to change it. Impossible is not a fact. It's an opinion. Impossible is not a declaration. It's a dare. Impossible is potential. Impossible is temporary. Impossible is nothing.”

–Muhammad Ali

THE TABLE OF CONTENTS

LIST OF FIGURES

ACKNOWLEDGEMENTS

Firstly, I would like to acknowledge Professor Andrea Tao for her support as the chair of my committee. Her guidance and encouragement has been incredibly invaluable to my growth as a researcher and engineer.

I would also like to acknowledge the entirety of Taolab, my fellow classmates, and good friends, without whom my academic tenure would have been exponentially longer, difficult, and boring. It is their support that has helped me in an immeasurable way.

Chapter 3, in full, is a reprint of the material as it appears in Chemical Communications. Gao, Bo, Yahya Alvi, David Rosen, Marvin Lav, and Andrea R. Tao., *Chemical Communications* 49, no. 39 (2013): 4382-4384. The thesis author was the second investigator of this publication.

Chapter 4, in full, has been submitted for publication in the CrystEngComm Journal. Gao, Bo, Yahya Alvi, Vincent Li, and Andrea R. Tao. The thesis author was the second investigator of this publication.

Chapter 5, Gurunatha Kargal, a postdoc in Taolab, was a crucial help with much of this work.

ABSTRACT OF THE THESIS

Designer Self Assembly: Distance, Coordination, and Orientation control of Plasmonic Nanoparticles

by

Yahya Mustafa Alvi

Master of Science in Nanoengineering
University of California, San Diego, 2014
Professor Andrea Tao, Chair

The ability to controllably assembly nanoscale building blocks into higher order architectures is crucial for the fabrication of functional materials and devices. Herein, we demonstrate the control of orientation, coordination, and interparticle distance of plasmonic nanoparticles through a polymer-assisted assembly mechanism. By modifying the shape and surface chemistry of the particles we were able to build homo- and hybrid plasmonic nanojunctions which can be used in high-resolution sensing and imaging, as well as enhancement of light absorption in photovoltaics.

1 Introduction to Self-Assembly of Plasmonic Nanoparticles

The emergence of nanotechnology has accelerated growth in many diverse industries such as medical diagnostics,[2-4] renewable energy,[5] drug delivery,[6-7] complex electronics,[8-9] and new materials[10] by providing unique solutions which couple functionality with size.[1] These advances do not involve single components, but rather rely on the engineering of whole nanosystems to give rise to highly specific functionalities. Nanomanufacturing of these modern devices involves extensive patterning of intricate components which are all working synchronously together. A great example is a common transistor used in most electronics which has a P-N junction capacitively coupled with a conductive gate through an oxide layer. Although it has four basic components, a typical microchip has almost a billion transistors on an integrated circuit backbone which communicates with each transistor.

A system such as this is usually fabricated using top-down lithographic techniques because they offer high precision and control for the fabrication of nanocomponents. Unfortunately, these techniques are usually limited by scalability, resolution, and cost. Development of spontaneous self-organization into well-defined structures, also known as self-assembly, is a critical next step in nanotechnology. It is a cost-effective alternative to top-down lithography and offers a versatile, facile, and scalable way to attain atomic feature sizes in devices which make use of the unprecedented physical and chemical properties of nanomaterials. Individual components can be synthesized cheaply in concentrated batches with high precision. Self-assembly utilizes intermolecular and interparticle forces to organize components through their

composition and environment, which allows this process to occur on any substrate in a massively parallel manner.

Many mechanisms have already been developed for inducing the assembly of nanoparticles. These include DNA-based strategies[11], bifunctional molecular linkers[12], electrostatic-induced assembly[13], and template assisted organization[14]. Most of these strategies tend to produce close-packed aggregates of structures with limited control on interparticle separation distance and nanoparticle coordination. In addition, as particle shape begins to deviate from traditional spherical components these strategies are unable to address control on interparticle orientation.

Several groups have been able to address these issues in gold nanorods by selectively modifying their tips with tethered polymer grafts. The nanorod tips have a less dense layer of stabilizing surfactant which can be easily displaced due to the high degree of curvature at the ends.[15] For example, Nie et al modified nanorod tips with hydrophobic polystyrene chains and this allowed them to control orientation based solely on solvent conditions.[16] However, this method relies solely on the ability that tip-selective surface modification can occur in nanorods. Facet selective modification on anisotropic nanoparticles with well-defined edges and faces, such as nanocubes, is much more difficult and requires the assistance of top down methods.[17, 18]

The use of DNA to dictate assembly is of great interest. In this method, single stranded DNA is grafted to the nanoparticle surface. In the presence of a particle grafted with the complimentary strand and proper ionic strength spontaneous assembly occurs as the DNA hybridizes. This method can be utilized to form tightly controlled spacing and packing geometries. In the work of Young et al. unique optical metamaterials were built

through the use of DNA dictating the 3-dimensional architecture of plasmonic nanoparticles.[19] One of the biggest challenges to DNA mediated assembly is that assembled structures possess very low particle volume fractions. A majority of the superlattice volume is occupied by water which renders the structure highly collapsible. Young et al, resolved this issue by back filling their assembled structures with silica by using aqueous silane chemistry. Although DNA offers high specificity and control, it is very limited by the structural density and integrity of the assembled architectures.

Our group is interested in the use of plasmonic nanoparticles to develop unique metamaterials by building and studying ensembles which display collective properties that are different from individual particles. Nanoparticles composed of noble metals, such as gold or silver, exhibit unique light-matter interactions that result in the excitation of plasmons. When conduction electrons are excited and begin to have a resonant interaction with incoming light, they coherently oscillate throughout the volume of the particle (Figure1.1). This results in highly intensified electric fields near the surface of the particle and can be utilized to trap and confine light to volumes smaller than the diffraction limit. Assemblies of such particles exhibit strong electromagnetic coupling which are of tremendous interest for applications in sub-wavelength optics and high resolution sensing.

This thesis concerns itself with discussing a polymer guided assembly approach of plasmonic nanoparticles which addresses spacing, orientation, and coordination.

Chapter 2 is a discussion on the synthesis and fabrication of our polymer-nanoparticle composite systems.

Chapter 3 concerns itself with the building of unique plasmonic homojunctions of nanoparticles.

Chapter 4 further expands our polymer guided assembly mechanism to understand and build plasmonic heterojunctions of nanoparticles.

Chapter 5 is the preliminary study in the use of DNA inside of a polymer matrix to assist assembly, as well as, a future perspective of the mechanism that we have developed.

1.1 Figures

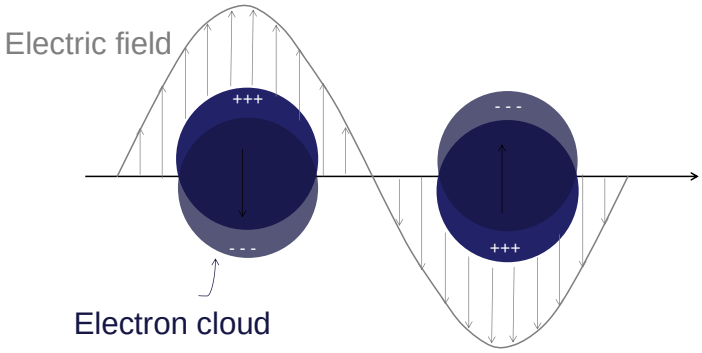

Figure 1.1. Cartoon of the plasmon excitation of the dipole mode in a spherical nanoparticle.

1.2 References

1. Bishop, K. J., Wilmer, C. E., Soh, S., & Grzybowski, B. A. (2009). *small*, *5*(14), 1600-1630.
2. M. Y. Han, X. H. Gao, J. Z. Su, S. Nie, *Nat. Biotechnol.* 2001, **19**, 631– 635.
3. M. M. C. Cheng, G. Cuda, Y. L. Bunimovich, M. Gaspari, J. R. Heath, H. D. Hill, C. A. Mirkin, A. J. Nijdam, R. Terracciano, T. Thundat,M. Ferrari, *Curr. Opin. Chem. Biol.* 2006, **10**, 11– 19.
4. Z. Wang, J. Lee, A. R. Cossins, M. Brust, *Anal. Chem.* 2005, **77**, 5770– 5774.
5. Sides, C. R., Li, N., Patrissi, C. J., Scrosati, B., & Martin, C. R. (2002). Nanoscale materials for lithium-ion batteries. *Mrs Bulletin*, *27*(08), 604-607.
6. M. Ferrari, *Nat. Nanotechnol.* 2008, **3**, 131– 132.
7. M. Ferrari, *Nat. Rev. Cancer* 2005, **5**, 161– 171
8. S. J. Tans, A. R. M. Verschueren, C. Dekker, *Nature* 1998, **393**, 49– 52.
9. Y. Cui, C. M. Lieber, *Science* 2001, **291**, 851– 853.
10. C. P. Collier, T. Vossmeyer, J. R. Heath, *Annu. Rev. Phys. Chem.* 1998, **49**, 371– 404.
11. Mirkin, C. A., Letsinger, R. L., Mucic, R. C., & Storhoff, J. J. (1996). *Nature*, *382*(6592), 607-609.
12. Pierrat, S.; Zins, I.; Breivogel, A.; Sönnichsen, C. Self-Assembly of Small Gold Colloids with Functionalized Gold Nanorods. *Nano Lett* **2007**, *7*, 259–263.
13. Gschneidtner, T. A.; Fernandez, Y. A. D.; Syrenova, S.; Westerlund, F.; Langhammer, C.; Moth-Poulsen, K. A Versatile Self-Assembly Strategy for the Synthesis of Shape-Selected Colloidal Noble Metal Nanoparticle Heterodimers. *Langmuir* **2014**, *30*, 3041–3050.
14. Zehner RW, Lopes WA, Morkved TL, Jaeger Hand Sita LR 1998 Langmuir 14241
15. N.R. Jana, L. Gearheart and C.J. Murphy, *Adv.Mater.* 2001, **13**, 1389–1393
16. Z. Nie, D. Fava, E. Kumacheva, S. Zou, G.C. Walker and M. Rubinstein, *Nat.Mater.*, 2007, **6**, 609–614
17. R. Sardar and J.S. Shumaker-Parry, *NanoLett.*, 2008, **8**, 731–736
18. B.B. Wang,B. Li,B. Zhao and C.Y. Li, *J.Am.Chem.Soc.*, 2008, **130**, 11594–11595
19. Young, Kaylie L., Michael B. Ross, Martin G. Blaber, Matthew Rycenga, Matthew R. Jones, Chuan Zhang, Andrew J. Senesi, Byeongdu Lee, George C. Schatz, and Chad A. Mirkin. *Advanced Materials* 26, no.4(2014):653-659.

2 Fabrication and Experimental Techniques

2.1 Introduction

Our group has developed a nanoparticle-polymer composite organization method in which interparticle distance, coordination, and orientation are addressed.[1,2] We have demonstrated that polymer-grafted shaped nanoparticles embedded within an immiscible polymer matrix assemble to form one-dimensional chain-like superstructures, after solvent or thermal annealing. This method results in assemblies with well-defined nanoscale junctions where interparticle orientation and distance is dictated by the length and miscibility of the polymer grafted onto the surface of the particle. The following chapter is the procedure for how our nanocomposites were made.

2.2 Experimental Methods

Nanoparticle synthesis and surface modification:

1. Synthesis of PVP- and PEG-grafted spherical Au NPs. Spherical Au NPs were synthesized according to the well-known Turkevich method.[3] The as-synthesized spherical Au NPs were then coated with poly(vinyl pyrrolidone) (PVP, M_w = 55k, Sigma-Aldrich) chains in aqueous solution under stirring as previously described.[4,2] Thiol terminated polyethylene glycol (PEG-SH, M_w = 20k, Laysan Bio) chains were grafted onto the citrate-capped Au NPs in aqueous solution using previously reported methods.[5] To remove excess polymer, the Au NPs were precipitated by centrifugation (Eppendorf Centrifuge 5804) and redispersed in ethanol. This process was repeated two times. The ligand exchange process was confirmed by UV-visible absorption spectroscopy, infrared spectroscopy, and dynamic light scattering.

2. Surface modification for polystyrene (PS)-grafted Au NPs. Surface modification of Au NPs was adapted from previously reported methods.[6] Specifically, 4 mL of as-synthesized citrate-capped NPs were centrifuged to precipitate the NPs, followed by redispersion of the NPs in 250 μL of DI H_2O. For functionalization with thiol-terminated polystyrene (PS-SH, M_w = 20k, Polymer Source), the aqueous Au NP dispersion was pipetted into 8 mL of a 2 mM PS-SH/tetrahydrofuran (THF) solution and stirred for 24 h. The resulting mixture was centrifuged and the precipitated Au NPs were redispersed in 10 mL of toluene. This step was repeated two additional times to remove unbound PS-SH molecules.

3. Ag nanocube synthesis. Ag nanocubes were synthesized using a previously reported polyol reaction.[7] Briefly, an $AgNO_3$ solution was prepared by sonicating 0.20 g $AgNO_3$ and 40 μL of 0.043 M $CuCl_2$ solution in 5 mL of 1,5-pentanediol until all the salt crystals were dissolved. A separate solution of polyvinyl pyrrolidone (PVP, M_w~55K) was prepared by dissolving 0.10 g PVP in 5 mL of 1,5-pentanediol. The growth solution was prepared by heating 20 mL of 1,5-pentanediol at 193°C. The $AgNO_3$ and PVP precursor solutions were alternately injected into the hot pentanediol at a rate of 500 μL/min and 320 μL/30 s, respectively. The injections were continued until the solution turned an opaque yellow color (after approximately 6 minutes), signaling the formation of nanocubes. The as-made nanocube was further purified by filtration and concentrated to the desired concentration in ethanol.[1,7]

4. Ag nanoprism synthesis. Ag nanoprisms were synthesized using a previous reported methods.[8,9] An aqueous solution of $AgNO_3$ (0.1 mM, 25 mL), trisodium citrate (30 mM, 1.5 mL), poly(vinylpyrrolidone) (M_w = 40,000 Da, 0.7 mM, 1.5 mL), and hydrogen

peroxide (30 wt%, 60 μL) is prepared and vigorously stirred at room temperature. Sodium borohydride (100 mM, 250 μL) is rapidly injected into the flask. After the addition of sodium borohydride the solution turns a pale yellow and after 30-45 minutes the solution changes to a blue color indicating the formation of silver nanoprisms. The free ligands in solution are removed by centrifuging 25 mL of the solution at 11000rpm for 8 min 2-3 times. Each time the particles should be redispersed in water. After the final wash, the particles should be redispersed in between 20-40 mL of water. The volume chosen should be based on color of the sample, if the prisms are too dilute they will destabilize and aggregate. 10 mL of the seed solution is then removed and stirred rapidly. To this solution L-ascorbic acid (0.1 M, 375 μL) and trisodium citrate (0.075 M, 125 μL) are added quickly. A separate solution was prepared by mixing 20 mL of $AgNO_3$ (1 mM), citric acid (0.1 M, 125 μL), and trisodium citrate (1.5 mM, 100 μL). This solution is added at a rate of 0.2 mL/min to the vigorously stirring seed solution. After 5 min, two thirds of the reaction solution was removed and the remaining solution was used as the new seeds for the next growth cycle.

5. Au nanorod synthesis. Au nanorods were synthesized using a previous reported seed mediated method.[10] 250 μL of a 0.01 M $HAuCl_4$ solution is added to 7.5 mL of a 0.1 M CTAB solution. Next, 600 μL of 0.01 M ice-cold sodium borohydride is rapidly added to the gold-CTAB solution. After turning brown, the resulting solution is maintained at room temperature for 2 hours. A 50 mL growth solution is prepared containing: 0.1 M CTAB, 0.4 mM $HAuCl_4$, 0.06 mM $AgNO_3$, and 0.64 mM Ascorbic Acid. Finally, 100 μL of the seed solution is added to this growth solution. The solution is allowed to react for 2-3 hours.

NP-polymer composite film fabrication and annealing: NP-polymer composite films were fabricated using previously reported methods for embedding NPs into supported polystyrene (PS, M_w=11000 Da) films.[19,20] The PS films were spin-coated onto clean Si substrates and possess film thickness ~180-200 nm as measured by atomic force microscopy (Veeco, Multimode Nanoscope IV). NP monolayers were formed at an air-water interface, then transferred onto the supported PS thin-films by dip-coating. For deposition of mixed NPs, each NP type was deposited individually from separately prepared NP monolayers. The nanoparticle-PS composite was then exposed to $CHCl_3$ vapor in a closed vessel at room temperature according to previous methods.[1,2,11,12] For monitoring the time-dependent evolution of assembly structures, the nanocomposite films were enclosed in individual vessels during the vapor exposure step and removed from the vessel after the desired time interval.

Sample characterization: Nanoparticle assemblies were characterized by scanning electron microscopy (SEM) using a FEI UHR Field Emission SEM equipped with a field emission cathode with a lateral resolution of approximately 2 nm. The acceleration voltage was between 10-20 kV.

2.3 References

1. B. Gao, G. Arya and A. R. Tao, Nat. Nanotech., 2012, **7**, 433-437.
2. Gao, B., Alvi, Y., Rosen, D., Lav, M., & Tao, A. R. (2013). Chemical Communications, 49(39), 4382-4384.
3. Turkevich, J.; Stevenson, P. C.; Hillier, J. A study of the nucleation and growth processes in the synthesis of colloidal gold. *Discuss. Faraday Soc.* **1951**, *11*, 55-75.
4. Correa-Duarte, M. A.; Pérez-Juste, J.; Sánchez-Iglesias, A.; Giersig, M.; Liz-Marzán, L. M. Aligning Au Nanorods by Using Carbon Nanotubes as Templates†. *Angew. Chem. Int. Ed.* **2005**, *44*, 4375–4378.
5. Manson, J.; Kumar, D.; Meenan, B. J.; Dixon, D. Polyethylene glycol functionalized gold nanoparticles: the influence of capping density on stability in various media. *Gold Bulletin* **2011**, *44*, 99-105.
6. Hore, M. J. A.; Frischknecht, A. L.; Composto, R. J. Nanorod Assemblies in Polymer Films and Their Dispersion-Dependent Optical Properties. *ACS Macro Lett.* **2012**, *1*, 115–121.
7. Tao, A.; Sinsermsuksakul, P.; Yang, P. Polyhedral Silver Nanocrystals with Distinct Scattering Signatures. *Angewandte Chemie International Edition* **2006**, *45*, 4597-4601.
8. Métraux, G. S., & Mirkin, C. A. (2005). Rapid thermal synthesis of silver nanoprisms with chemically tailorable thickness. *Advanced Materials*, *17*(4), 412-415.
9. Zhang, Q., Hu, Y., Guo, S., Goebl, J., & Yin, Y. (2010). Seeded growth of uniform Ag nanoplates with high aspect ratio and widely tunable surface plasmon bands. *Nano letters*, *10*(12), 5037-5042.
10. N. R. Jana, L. Gearheart and C. J. Murphy, Adv. Mater., 2001, 13, 1389–1393.
11. Akcora, P.; Liu, H.; Kumar, S. K.; Moll, J.; Li, Y.; Benicewicz, B. C.; Schadler, L. S.; Acehan, D.; Panagiotopoulos, A. Z.; Pryamitsyn, V.; Ganesan, V.; Ilavsky, J.; Thiyagarajan, P.; Colby, R. H.; Douglas, J. F. Anisotropic self-assembly of spherical polymer-grafted nanoparticles. *Nat. Mater.* **2009**, *8*, 354-359.
12. Hooper, J. B.; Bedrov, D.; Smith, G. D. Supramolecular self-organization in PEO-modified C60 fullerene/water solutions: Influence of polymer molecular weight and nanoparticle concentration. *Langmuir* **2008**, *24*, 4550-4557.

3 Designer Nanojunctions: Orienting Shaped Nanoparticles within Polymer Thin-film Nanocomposites

3.1 Introduction

Noble metal nanoparticles (NP) that support localized surface plasmon resonances have attracted attention due to their ability to control and manipulate light at nanoscale dimensions. Research efforts have been made toward organizing shaped NPs into hierarchically ordered structures such as extended NP superlattices, arrays, and networks.[1-3] In many cases, highly one-dimensional (1D) superstructures of metal NPs with nanometer-sized interstitial gaps are desired. Within the nanojunction gap formed by neighboring NPs, the electromagnetic field is highly intensified due to light confinement. The degree and manner of light confinement depend dramatically on the interparticle orientation and gap distance for the nanojunction, and are of great importance for applications such as surface-enhanced Raman spectroscopy and metamaterials.

Self-assembly can enable the large-scale fabrication of nanojunction arrays through the organization of metal NPs within polymer films. We previously demonstrated that polymer-grafted metal NPs embedded within a polymer matrix can undergo self-assembly and self-orientation without any face-selective chemical modification of the NP surface.[4]Silver nanocubes grafted with hydrophilic polymers were organized into arrays of 1D strings within a hydrophobic polystyrene matrix film. This nanocomposite blend could be fabricated over large areas (> 6 cm^2) using either thermal or solvent annealing to trigger spontaneous phase separation of NP and polymer components.[2] Depending on the length of the grafted polymer chain, nanocubes could be assembled through either edge-edge or face-face interactions by tailoring the attractive

van der Waals (vdW) and repulsive steric forces between neighboring NPs.

Here, we apply this facile self-assembly approach to a variety of metal NP shapes, including spherical NPs, nanorods, and triangular nanoprisms. These NPs possess highly regular shapes that have the potential to result in nanojunctions with specific coordination geometries (e.g. linear or trigonal assemblies) based on their number of vertexes as depicted in Figure 3.1. Nanospheres possess no vertexes, nanorods possess two vertexes, and nanoprisms possess three vertexes, all with the potential to self-assemble into string or island like superstructures upon nanocomposite phase separation. These NPs also possess unique surface plasmon resonance signatures that correspond to their shape, making them ideal candidates for constructing nanojunctions with tailored plasmonic properties.

During the assembly process, NP orientation is dictated by two factors, as established by our earlier work on silver nanocubes: the directional interparticle interactions provided by the NP shape and the chain length of the grafted polymer.[4] "Bare" metal nanoparticles are expected to experience a net attractive potential for assembly due to vdW forces. Polymer grafts introduce steric repulsion between two closely-spaced nanoparticles, generated by chain compression as the nanoparticles approach with each other. These repulsion forces can be modulated by chain length. When grafted with short polymer chains, the NPs adopt side-side orientations favored by strong vdW interactions. When grafted with long polymer chains, the NPs favor vertex-vertex orientation which alleviates the steric repulsion between adjacent, closely-spaced NPs.

3.2 Experimental Methods

These have been laid on in Chapter 2.

3.3 Results and Discussion

First, we demonstrate the assembly of spherical NPs within a homopolymer matrix (Fig. 3.2a) We synthesized well-dispersed spherical gold NPs (diameter = 13 nm) according to Turkevich method.[5] The NPs were coated with a long polymer graft of poly(vinyl pyrrolidone) (PVP) with a M_w = 55k and a final graft layer thickness of 15 ± 1 nm as measured by dynamic light scattering. The NPs were then distributed at an air-water interface to facilitate transfer onto a supported polystyrene (PS, M_w = 11k) thin-film. Upon exposure to chloroform vapor, the well-separated nanoparticles (Fig. 3.2c) sink into the hydrophobic polymer matrix. This is followed by spontaneous phase segregation into 1D superstructures that are a single-NP wide (Fig. 3.2d). Because the spherical NPs are totally isotropic in shape and surface chemistry, the formation of these string structures is somewhat surprising. Previous reports for polystyrene grafted silica nanopheres (diameter = 14 nm) have suggested that these superstructures are achieved through dipole-like interactions caused by rearrangement of the polymer grafts at the NP surface.[1, 6] These studies demonstrated that polymer graft length is a key parameter in dictating superstructure morphology, which can be modulated from aggregates to sheets to strings.[1, 7] To demonstrate the importance of the polymer graft length in our nanocomposite system, we grafted the spherical gold NPs with a short polymer graft composed of (11-mercaptoundecyl) tetra (ethylene glycol). This alkanethiol is terminated with a short four-unit PEG chain with a total chain length of approximately 2.0 nm.[8] Upon solvent annealing, these NPs form island-like clusters during the phase segregation process (Fig. 3.3e). This higher NP packing density is consistent with a decrease in steric

repulsion between the polymer grafts attached to neighboring NPs.

Next, we demonstrate the oriented assembly of gold nanorods, which are known to display dipolar surface plasmon resonances corresponding the long and short axes of the nanorod.[9] Nanorods have been widely explored as building blocks for extended chains and network structures in both polymer blends and within colloidal dispersions.[10-12] Here, we show that nanorods can be assembled with tip-tip orientations in a homopolymer matrix and without site-selective chemical functionalization. (Fig. 3.3) Gold nanorods (12 nm wide and 45 nm long) were synthesized by seed-mediated growth[13] and coated with long PVP polymer chains (M_w = 55K). The phase segregation process results in the assembly of nanorods into extended 1D superstructures (Fig. 3.3b and c) where 82.1 ± 1.0 % of the assembled nanorods adopt tip-tip (TT) orientations and 9 ± 1.6 % adopt side-side (SS) orientations.

The slow diffusion rate of nanorods in the high viscosity polymer matrix allows us to carry out time-dependent observations of the assembly process. We analyzed nanorod-polymer composite films at different stages of assembly by removing films from the solvent vapor, which effectively solidifies the polymer matrix and traps the dynamic 1D superstructures. At early stages of 1D string formation, well-separated nanorods aggregate to form short chains consisting of only a few nanorods (Fig. 3.3b). As assembly proceeds, these short chains grow by merging with neighboring chains (Fig. 3.3c). This is different from other mechanisms where strings nucleate and slowly grow through the end-attachment of single nanorods.[14] To demonstrate the influence of the graft polymer on nanorod orientation, we modified the gold nanorods with short PEGylated alkanethiol grafts. As shown in Fig. 3.3e when these PEGylated nanorods are

assembled within the homopolymer composite, they adopt the SS configuration with a 46.3 ± 2.9 % occurrence and the TT configuration with a 33.4 ± 2.1 % occurrence. The nanorod chains are composed of linked nanorods bundles that are 2-3 NPs thick, which we attribute to the reduced steric repulsion stemming from the shorter grafts. In contrast with our previous observations for nanocubes, the relatively low ratio of SS-oriented nanorods is likely due to kinetically trapped orientations. We suspect that rotation is severely limited by the high aspect-ratio of the nanorods (~3.8) and that the nanorods possess a high energy barrier for reorientation. This is evidenced by nanocomposite films that were subjected to thermal annealing above T_g of the polystyrene matrix and do not exhibit signs of nanorod reorientation or reordering (Fig. 3.3f).

We also demonstrate the oriented assembly of silver triangular nanoprisms, which we expect to form hierarchical superstructures dominated by vertex-vertex NP orientations. The nanoprisms (side length = 250 nm and thickness =10 nm) were synthesized by colloidal methods.[15] We carried out surface modification of the nanoprisms with a long thiol-terminated polyethylene glycol (PEG) graft (M_w = 54k) and deposited the prisms onto a supported polystyrene film (Fig. 3.4a). Upon solvent annealing, nanoprisms assemble into string-like structures. Coordination through nanoprism vertexes (Fig. 3.4b) are favored, with 52.1 ± 2.0 % of the nanojunctions resembling bow-tie junctions. Reorientation of the prisms into side-by-side orientations can be promoted with a shorter polymer graft, where these orientations are observed with a 49.8 ± 1.7 % occurrence.

Many of the triangular nanoprisms appear to be trapped in orientations where the nanoprisms are rotated off of the junction axis. We account for these defects by

considering the nanoprism geometry. First, the nanoprism shape does not allow for high polymer compression. Because the nanoprisms are quite thin, polymer chains are able to escape physical confinement within the nanoparticle junction, leading to alleviated steric repulsion during the assembly process. Thus, tailoring graft length may not modulate nanoprism interactions as effectively as with other shapes. Second, many of these defect orientations are caused by imperfections in shape. For example, nanoprisms synthesized by colloidal methods are known to possess highly rounded corners. Polymers grafted to vertexes with a larger radius of curvature experience less steric repulsion upon assembly, which can lead to misorientation. However, these defects have the potential to be ameliorated by introducing additional attractive or repulsive interactions between grafted chains and the nanoprism surface.

3.3 Conclusions

In summary, we demonstrate the ability to fabricate large-area nanocomposites where metal NPs of varying size, shape, and valence spontaneously organize into oriented nanojunctions. The nature of this NP assembly is highly dependent on NP-polymer interfacial interactions and interparticle interactions, and the presence of assembly defects or misorientation can be attributed directly to NP building block dimensions. This approach is highly versatile with the potential to be extended towards non-metallic NPs such as semiconductor quantum dots or dielectric NPs, facilitating fabrication of engineered nanocomposites that exhibit well-defined structure-property relationships.

3.4 Figures

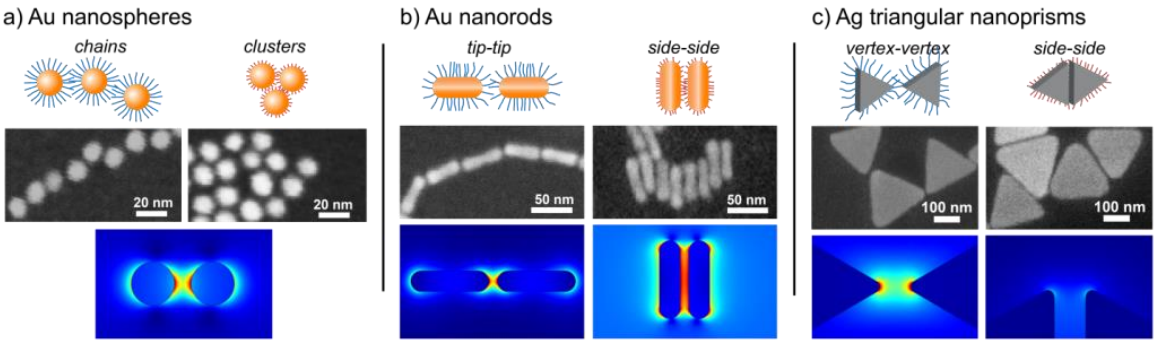

Figure 3.1. Schematics, SEM images, and electrodynamic simulations of (a) Au nanosphere, (b) Au nanorod, (c) Ag triangular nanoprism assemblies. The color scale for the simulation results correspond to electromagnetic near-field amplitude (E) with respect to the incident field, E_o when excited at the resonant surface plasmon frequencies. Dark blue corresponds to E = 0 V/m and red corresponds to an E of (a) $17E_o$ for spheres, (b)130 E_o for tip-tip nanorods and $4.5E_o$ for side-side nanorods, and (c) $2000E_o$ for both vertex-vertex and side-side nanoprisms.

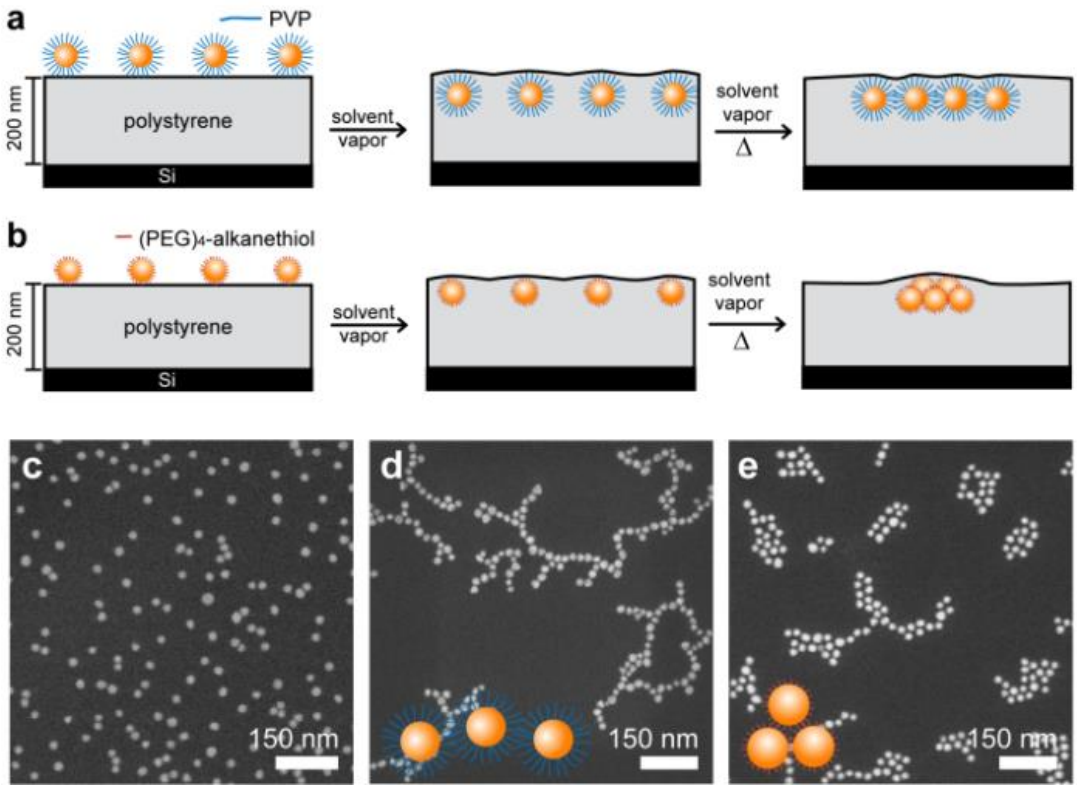

Figure 3.2. Schematic of Au nanosphere self-assembly in PS film upon solvent annealing. (a) Long-chain PVP-coated Au NPs embed and self-assemble into string like structures; (b) Short-chain $(PEG)_4$ alkanethiol coated Au NPs embed and self-assemble into cluster like structures. SEM images of (c) Au NPs deposited on PS film before anneal; resulting films of Au NPs coated with (d) long PVP chains and (e) short $(PEG)_4$-alkanethiols.

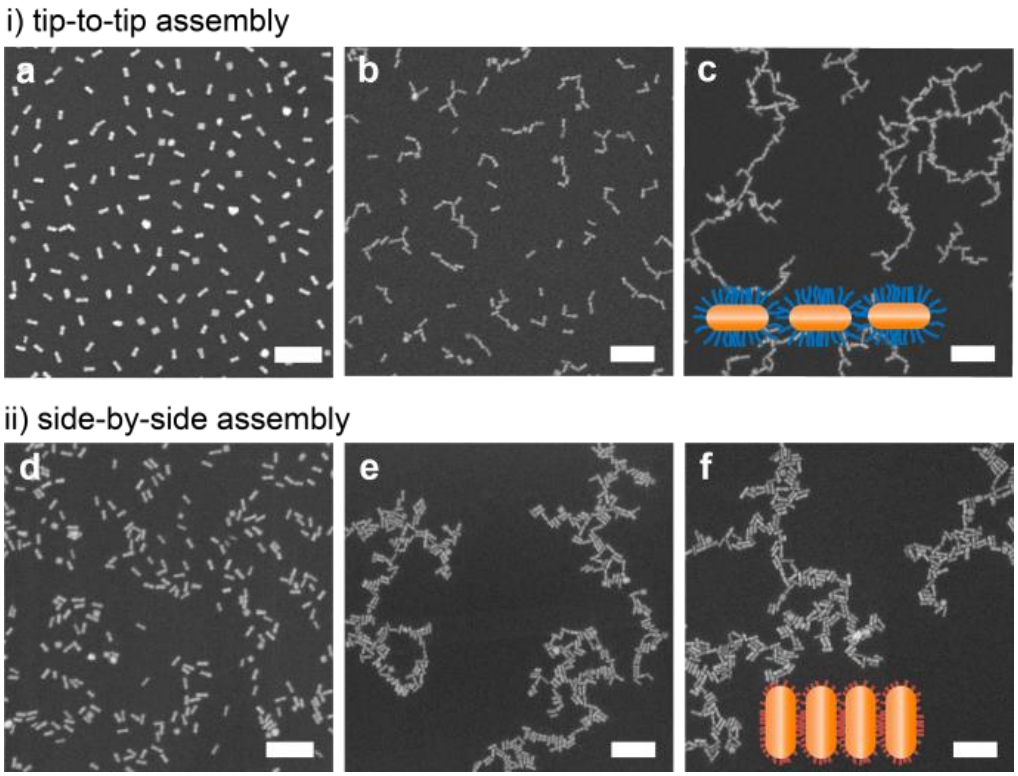

Figure 3.3. SEM images of assembled Au nanorods. Long-chain PVP-coated nanorods after solvent annealing for (a) 0 min and (b) 110 min. (c) SEM image of the network formed at high nanorod loading density. Short $(PEG)_4$-alkanethiol coated nanorods (d) before annealing, (e) after solvent annealing for 145 min and (f) heated for 4 hrs at 110˚C after solvent annealing to form side-to side NP aggregates. Scale bar is 200 nm.

3.5 References

1. P. Akcora, H. Liu, S. K. Kumar, J. Moll, Y. Li, B. C. Benicewicz, L. S. Schadler, D. Acehan, A. Z. Panagiotopoulos, V. Pryamitsyn, V. Ganesan, J. Ilavsky, P. Thiyagarajan, R. H. Colby and J. F. Douglas, *Nat. Mater.*, 2009, **8**, 354-359.
2. S. C. Glotzer and M. J. Solomon, *Nat. Mater.*, 2007, **6**, 557-562.
3. Z. Nie, A. Petukhova and E. Kumacheva, *Nat. Nanotech.*, 2009, **5**, 15-25.
4. B. Gao, G. Arya and A. R. Tao, *Nat. Nanotech.*, 2012, **7**, 433-437.
5. J. Turkevich, P. C. Stevenson and J. Hillier, *Discuss. Faraday Soc.*, 1951, **11**, 55-75.
6. J. B. Hooper, D. Bedrov and G. D. Smith, *Langmuir*, 2008, **24**, 4550-4557.
7. D. Maillard, S. K. Kumar, A. Rungta, B. C. Benicewicz and R. E. Prud'homme, *Nano Letters*, 2011, **11**, 4569-4573.
8. B. Zhu, T. Eurell, R. Gunawan and D. Leckband, *Journal of Biomedical Materials Research*, 2001, **56**, 406-416.
9. K. G. Thomas, S. Barazzouk, B. I. Ipe, S. T. S. Joseph and P. V. Kamat, *The Journal of Physical Chemistry B*, 2004, **108**, 13066-13068.
10. J. A. H. Michael and L. Mohamed, *Prospects of nanorods as an emulsifying agent of immiscible blends*, AIP, 2008.
11. Z. Nie, D. Fava, E. Kumacheva, S. Zou, G. C. Walker and M. Rubinstein, *Nat. Mater.*, 2007, **6**, 609-614.
12. K. Liu, N. Zhao and E. Kumacheva, *Chem. Soc. Rev.*, 2011, **409**, 656-671.
13. N. R. Jana, L. Gearheart and C. J. Murphy, *Adv. Mater.* , 2001, **13**, 1389-1393.
14. K. Liu, Z. Nie, N. Zhao, W. Li, M. Rubinstein and E. Kumacheva, *Science*, 2010, **329**, 197-200.
15. G. S. Métraux and C. A. Mirkin, *Adv. Mater.*, 2005, **17**, 412-415.

Chapter 3, in full, is a reprint of the material as it appears in Chemical Communications. Gao, Bo, Yahya Alvi, David Rosen, Marvin Lav, and Andrea R. Tao., *Chemical Communications* 49, no. 39 (2013): 4382-4384. The thesis author was the second investigator of this publication.

4 Polymer-Directed Assembly of Colloidal Nanoparticle Heterojunctions

4.1 Introduction

The controlled assembly of multiple types of nanoparticles (NPs) that possess different sizes, shapes, or compositions into hybrid nanocomposites remains a considerable challenge for the fabrication of functional nanomaterials and nanodevices.[1] Ensembles of different functional NPs (e.g. plasmonic, photoluminescent, dielectric, and magnetic) that exhibit collective NP interactions have the potential to enable novel and unexplored physical phenomena.[2,3] For example, Ag and Au NPs with unique localized surface plasmon resonances can be assembled into clusters that exhibit strong electromagnetic coupling between NPs and are of tremendous interest for applications in subwavelength optics[4,5] and sensing.[6] Assymmetric nanojunctions formed by coupling two different plasmonic NPs have been utilized in the fabrication of a nanojunctions that exhibit exceptionally high light confinement and or exhibit unique Fano resonances.[7,8] A dimer composed of one Au NP and one Ag NP was demonstrated to exhibit electromagnetic coupling of the Ag NP's surface plasmon resonances to the interband transitions belonging to the Au NP.[9,10] Heterojunctions composed of one plasmonic NP and a non-plasmonic NP are also desired. For example, coupling a metal NP to a semiconductor quantum dot is desired for enhanced photoluminescence or for observing energy transfer processes.[11,12] The generation of a heterojunction between an Ag NP and a surface-active NP (such as Pd or ZnO) has been reported to give increased photocatalytic activity. [13,14]

To pursue the fabrication of these heterostructures, several methodologies have been developed for inducing NP assembly, including DNA-based strategies, [2,9,15] bifunctional molecular linkers, [16] and electrostatic-induced assembly between nanoparticles with different charges.[17] However, controlling the interparticle separation distance and the manner in which NPs coordinate can be difficult. Most of these strategies tend to produce close-packed or jammed structures. In addition, NP shape poses additional challenges in generating heterostructures since interparticle orientation must also be considered.[18] Previously, we demonstrated that polymer-grafted shaped NPs embedded within an immiscible polymer matrix assemble to form one-dimensional (1D) chain-like NP superstructures.[19,20] Phase segregation of these superstructures is induced by solvent or thermal annealing. This method results in NP assemblies with well-defined nanoscale homojunctions where interparticle orientation is dictated by the length and miscibility of the polymer graft. For Ag nanocubes grafted with long hydrophilic polymers, the generation of NP homojunctions produces a highly intensified electromagnetic field to form plasmonic "hot spots."

In this work, we further extend this polymer-directed assembly strategy to construct NP heterojunctions composed of NPs that possess different shapes, sizes, and compositions. We examine the rate of NP assembly within a polymer matrix and demonstrate how co-assembly can carried out using a binary mixture of NPs. The self-organization of NP heterojunctions is dictated by the diffusion rate of each type of NP within the polymer matrix, relative NP density, and miscibility of the polymer graft.

4.2 Experimental Methods

These have been explained in Chapter 2.

4.3 Results and Discussion

Figure 4.1 shows a schematic of the assembly process and SEM images of the assembly structures obtained from individual NP building blocks. Spherical Au NPs (*d*=21± 2 nm) and Ag nanocubes (*e*=80± 4 nm) were embedded into a hydrophobic PS thin-film, and phase segregation was carried out by solvent vapour exposure. Both the Au NPs and Ag nanocubes are grafted with hydrophilic PVP ligands and assemble into anisotropic chain-like structures, consistent with our previous observations.[19,20] Solvent annealing enables NP migration, rotation, and redistribution within the PS thin-film by swelling the PS chains to form a glassy, molten matrix. PS serves as a convenient medium to capture any dynamic NP superstructures because removing the nanocomposite film from solvent vapor causes the polymer film to harden. Here we take advantage of this to monitor the NP assembly and the structures that form during phase segregation by removing the NP-loaded films from solvent vapor after various time intervals to carry out SEM analysis.

Nanocomposite films were fabricated by loading Au NPs into PS with a surface density ϕ=270 NPs/μm^2, which corresponds to a surface coverage of 9.01 ± 0.57%. (Figure 4.1b-e) In the early stages of solvent annealing, the NPs sink vertically into the PS film (which was confirmed by AFM) and show no signs of lateral diffusion up to 75 min of solvent vapour exposure. After 95 min, the NPs assemble into small clusters consisting of 2-3 NPs. These clusters then grow into longer NP chains through the attachment of both single NPs and neighboring NP chains. SEM images show that chain growth occurs as the population of individual NPs decreases. After 135 min, NP chain growth appears to be dominated by discrete chains that merge to form branched

superstructures. While the NPs form larger clusters in a few regions, the majority of the structures are comprised of chains that are only a single NP wide. The overall NP density in the PS film remains constant during the assembly process, and chain merging continues until the surrounding supply of NPs is depleted. As a result, the final lengths of the Au NP chains are strongly dependent on the initial NP loading density prior to assembly.

Figure 4.1e-h shows the self-assembly process for nanocomposites composed of Ag nanocubes embedded in a PS thin-film with a NP loading density ϕ=11-12 cubes/μm^2, corresponding to a surface coverage of 7.68 ± 0.51%. Because the Ag nanocubes are considerably larger than the Au NPs, the required solvent annealing time (135 min) to embed the nanocubes into the PS matrix is considerably longer than the time required for Au NPs. After 150 min, Ag nanocubes are observed to assemble into small clusters, which continue to grow into longer chain-like structures with similar assembly kinetics. We did not pursue solvent annealing times longer than 180 min due to polymer dewetting from the underlying solid support, evidenced by the emergence of small pinholes at the surface of the nanocomposite film.

To fabricate heterojunctions composed of both spherical Au NPs and Ag nanocubes, we take advantage of the different time windows for self-assembly observed for the two NPs. (Figure 4.2a) To facilitate co-assembly, a mixture of Au NPs and Ag nanocubes was deposited onto a PS thin-film (Figure 4.2b). Upon exposure to chloroform vapour for 115 min, the Au NPs are the first to sink into the PS and being to assemble into small clusters. In Figure 4.2c, we observe the formation of short NP chains composed exclusively of spherical Au NPs (homojunctions) and short NP chains attached

to Ag nanocubes (heterojunctions). After 130 min, the Au NP chains have grown longer by depleting most of the single NPs and merging of small clusters. Most of the Ag nanocubes, which have not begun to assemble, have Au NPs attached to their corners. After 150 min, the Ag cubes with attached Au NP chains begin to diffuse laterally within the PS matrix and coalesce with other sphere-cube assemblies. After 170 min, these assemblies form branched structures where the Ag nanocubes serve as "joints" for the extension of Au NP chains.

Figure 4.2h shows the optical extinction spectra for individual Ag nanocube (black line) and Au nanosphere (red line) assemblies after annealing. Optical scattering from the Ag nanocube assembly is significantly higher in intensity than the Au nanoparticle assemblies, which is attributed to their larger size and the larger scattering cross-section of Ag. Nanocube assemblies, as previously reported, show a broad feature in the 800-1000 nm range which is attributed to the formation of edge-to-edge homojunctions and the resulting dipole-dipole coupling between neighboring Ag nanocubes. This is further confirmed when the optical response of the nanocube assembly is compared to the optical response of colloidal Ag nanocubes that are isotropically distributed in water (blue line, Fig. 4.2i), which exhibits no spectral peak in this wavelength region. Figure 4.2i shows the spectrum of co-assembled Ag nanocubes and Au nanospheres (red line). The optical response of the co-assembled nanoparticles appears very different from the individual cube and sphere nanocomposites, and does not display any spectral evidence of significant plasmonic coupling between Ag nanocubes. Rather, the optical response of the coassembly resembles the spectrum for isotropically distributed Ag nanocubes and shows good registry with the spectral features obtained for

isotropically distributed nanocubes. Compared to the colloidal Ag nanocubes, a small red-shift (10-30 nm) in the spectral peaks of the assembly is attributed to the presence of the polymer matrix, which possesses a higher refractive index than water. In addition, the spectrum for the coassembly exhibits a spectral shoulder near 700 nm, which we attribute to scattering from assembled Au nanospheres. These results suggest that co-assembly may provide a unique method for retaining isotropic nanoparticle distribution within a polymer composite to combat phenomena such as composite aging and particle aggregation.

Figure 4.3 shows a schematic of how the resulting sphere-cube chains can be viewed as NP analogue of copolymer chains, where Ag nanocubes serve as one monomer (A) and Au NP as another monomer (B). The overall composition of the NP copolymer chain is dependent on the initial relative loading density of each NP. Figure 4.3b-d shows heterojunctions obtained for nanocomposites with a sphere-to-cube loading densities of approximately: a) 40:1 (high), b) 20:1 (medium), and c) 10:1 (low). We observe that the main difference between these structures is the average distance between cubes, corresponding to the size of bridging Au NP blocks. By tuning the loading density of Au NPs, distance between assembled cubes can be readily tuned which may provide a strategy for tuning plasmonic properties of the composite film. At very high loading densities of spherical NPs, we observe that the average intercube distance remains very close to the initial intercube distance prior to solvent annealing. This co-assembly process may provide a strategy for stabilizing nanocomposite structures where the dispersity of a single nanocomponent is critical for material performance. However, this co-assembly

process is dictated by i) the relative diffusion rates, and ii) the sticking probabilities of each NP.

For example, if NPs possess a similar diffusion rate, the resulting NP assemblies possess similar rate of assembly and the resulting NP chains exhibit structure that reflect equal incorporation of the NPs. Figure 4.4a shows this for Ag nanocubes and Ag triangular nanoprisms with *e*=115 nm. Upon loading into the PS matrix at near-equivalent loading densities, co-assembly from mixtures of the two building blocks results in chains of alternating NPs. On the other hand, when the NPs possess different sticking probabilities (defined as the likelihood that a collision with another NP will produce a NP junction), the structure of the resulting NP chain can be significantly altered due to the different interparticle interactions. Figure 4.4b shows SEM images for co-assembly between Ag nanocubes and Au NPs where the Au NPs are grafted with thiol-terminated PS (M_w = 20k). Due to the miscibility between the grafted PS and the PS matrix, the Au NPs exhibit much lower sticking probabilities and do not form homojunctions with other Au NPs. However, van der Waals attraction between the cubes and spheres are sufficiently strong such that sphere-cube heterojunctions are formed. Because interactions between the graft polymers attached to the two different NP building blocks is unfavorable, the overall attractive cube-sphere interaction is relatively weak. In most cases, heterojunction formation is stabilized by one sphere coordinated between the adjacent facets of two nanocubes. This is confirmed by the large separation distance observed between the Au NPs and the Ag nanocubes, which is measured to be 16±1 nm. This is consistent with the estimated radius of gyration of the PS grafts (~10 nm) and PVP grafts (~ 4 nm), indicating that little-to-no interdigitation occurs between

the polymer grafts of cubes and spheres. In this case, increasing the sphere-to-cube loading density has little effect on the final morphology of the assembled chain and we observe that several Au NPs remain unassembled in the nanocomposite even after extensive solvent annealing.

4.4 Conclusion

In summary, we use a polymer-directed approach to fabricate nanocomposites that are comprised of co-assembled NPs with varying size, shapes, composition and polymer grafting chemistries. NP heterojunctions can be formed by taking advantage of the diffusion-limited assembly mechanism exhibited by polymer-grafted NPs within polymer matrices, utilizing NPs that exhibit different diffusion rates. The composition and morphology of the resulting NP co-assemblies can be further tuned by controlling the ratio of NP loading densities, relative NP sizes, and polymer graft miscibility. This method enables the fabrication of self-assembled structures comprised of multiple nanoscale building blocks, especially the plasmonic heterojunctions which could be important for fundamental studies of plasmonic properties that are caused by the asymmetry of nanostructures with unequally sized building blocks.

4.5 Figures

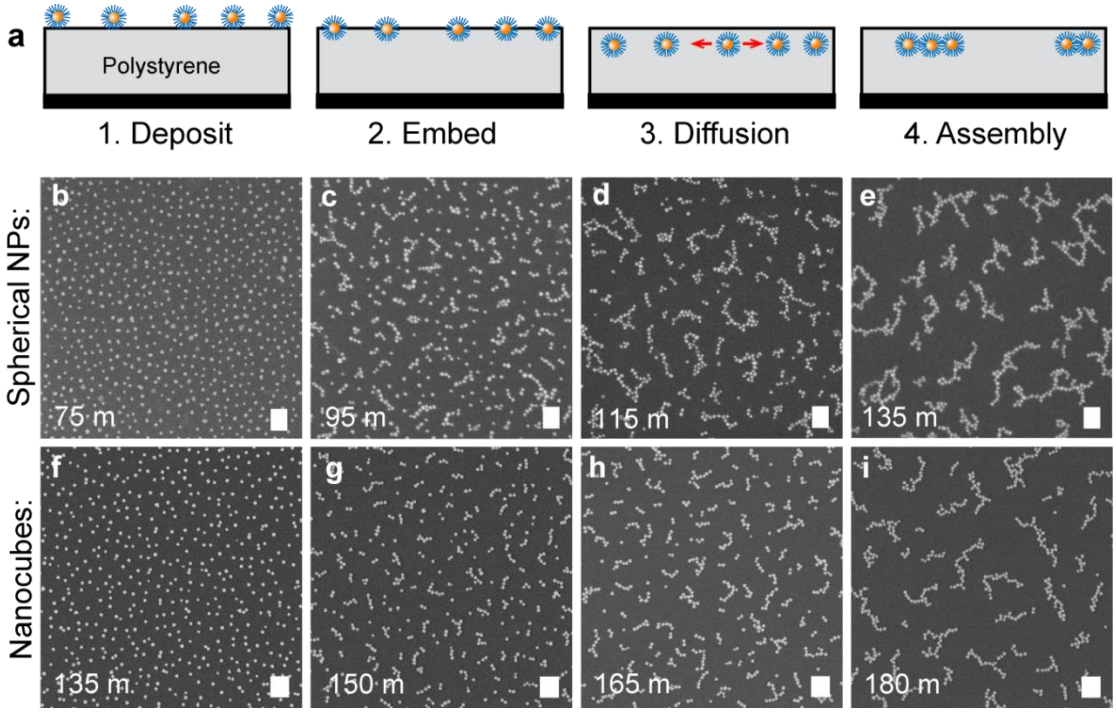

Figure 4.1. Dynamic assembly structures of nanocubes and nanospheres incorporated into a supported polymer thin-film. (a) Schematic of the self-assembly process. (b-i) SEM images showing the evolution of (a-d) Au nanospheres (scale bar = 200 nm) and (e-h) Ag nanocubes (scale bar= 500 nm) assembly structures upon solvent annealing.

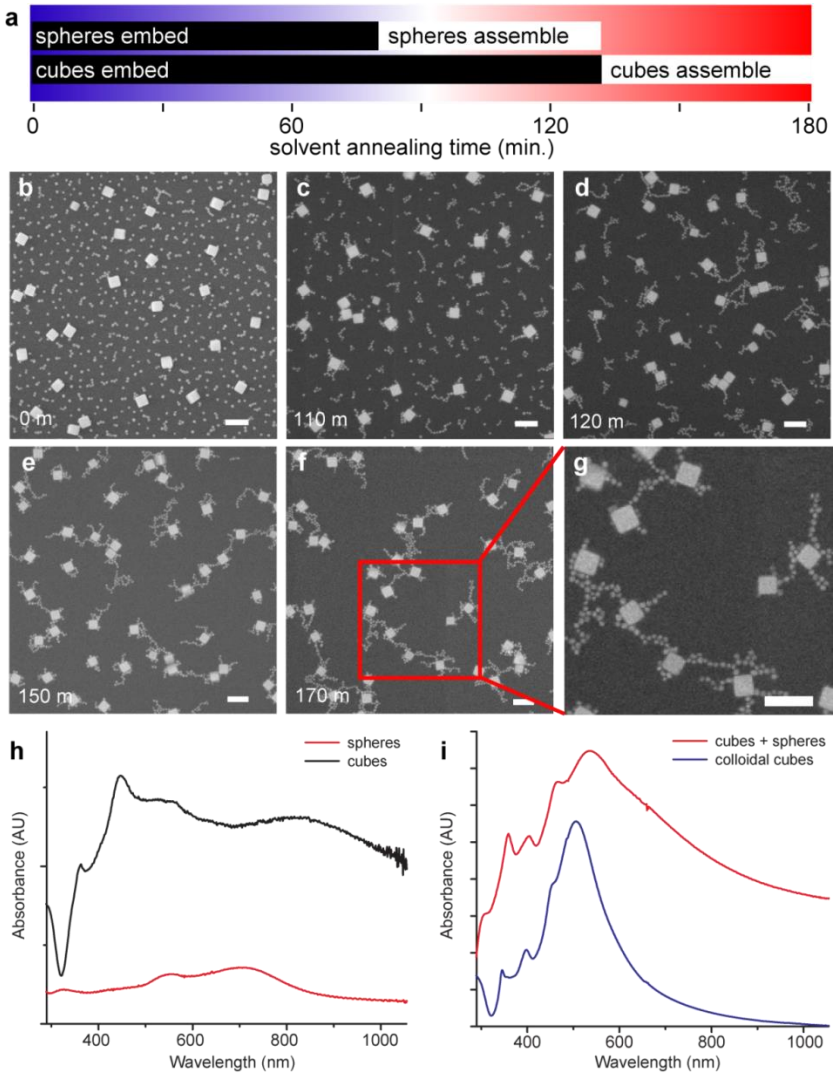

Figure 4.2. Co-assembly of spheres and cubes. (a) Timeline of the assembly process during solvent annealing of the nanocomposite film, showing that spherical nanoparticle embed and assemble prior to the initiation of nanocube assembly. (b–f) SEM images of mixed nanocube and nanosphere assemblies upon solvent annealing for different time intercals. (g) SEM image showing a close-up view of the co-assembled structure. (h) Extinction spectra for assembled Ag nanocube and Au nanosphere nanocomposites. (i) Extinction spectra for a co-assembled nanocube and nanosphere composite and for a an aqueous colloidal nanocube dispersion. All scale bars = 200 nm.

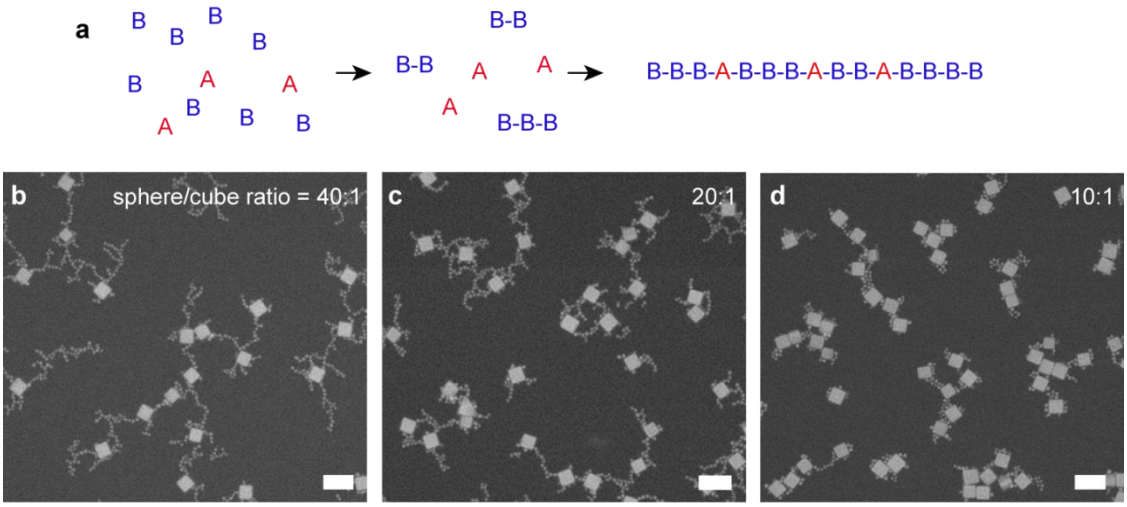

Figure 4.3. (a) Schematic of copolymerization between two different monomers, labelled as A and B. SEM images of co-assembled structures with approximate sphere/cube loading ratios of (b) 40:1, (c) 20:1 and (d) 10:1.

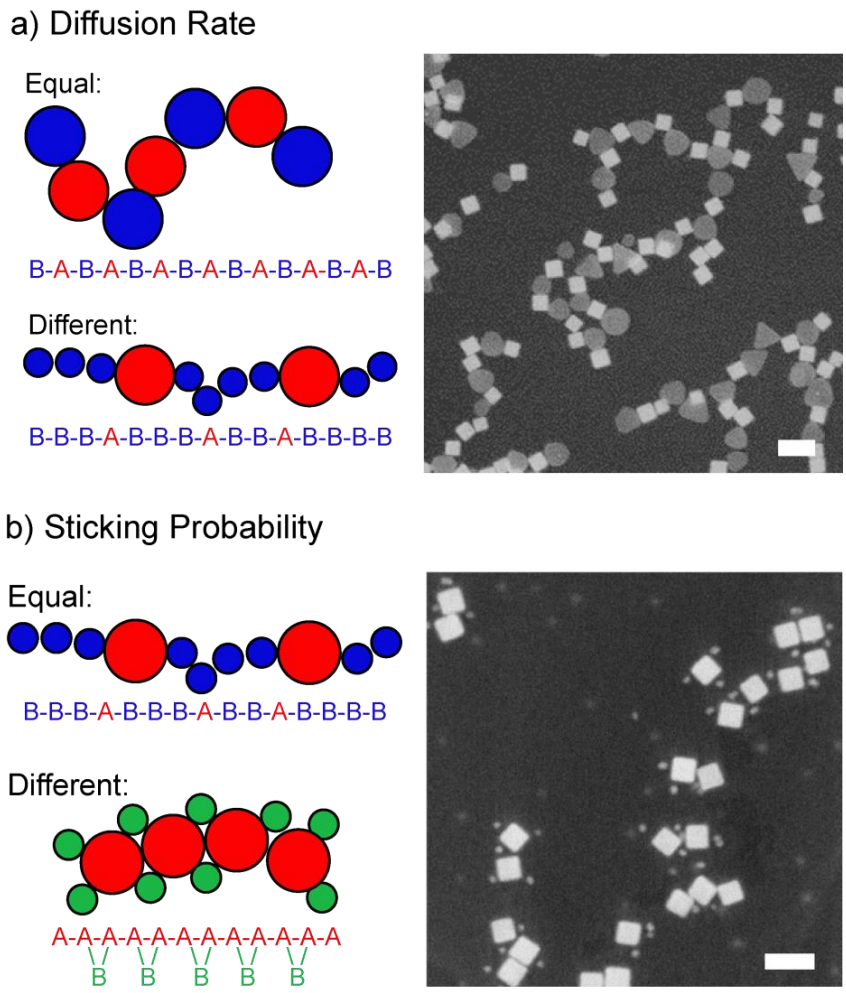

Figure 4.4. Schematic and SEM images of co-assemblies for particles with varying (a) diffusion coefficients, and (b) sticking probabilities. (a) Nanoparticles that exhibit similar in-polymer diffusion rates should assemble into structures that reflect their relative loading densities, as seen in with Ag nanocubes and Ag nanoprisms with similar sizes. Triangular Ag nanoplates possess an edge length=115 nm and are grafted with long-chain PEG thiol ligands. (b) Nanoparticles that exhibit different in-polymer miscibilities are expected to possess different sticking probabilities. The SEM image shows the resulting structure obtained for polystyrene miscible Au nanospheres (diameter=21 nm) and immisicible Ag nanocubes. The nanospheres are grafted with a long-chain PS-thiol ligand. All scale bars = 200 nm.

4.6 References

1. Bishop, K. J. M.; Wilmer, C. E.; Soh, S.; Grzybowski, B. A. Nanoscale Forces and Their Uses in Self-Assembly. *Small* **2009**, *5*, 1600- 1630.
2. Zhao, Y.; Xu, L.; Liz-Marzan, L. M.; Kuang, H.; Ma, W.; Asenjo-Garcia, A.; Javier Garcia de Abajo, F.; Kotov, N. A.; Wang, L.; Xu, C. Alternating Plasmonic Nanoparticle Heterochains Made by Polymerase Chain Reaction and Their Optical Properties. *Journal of Physical Chemistry Letters* **2013**, *4*, 641-647.
3. Wen, F.; Ye, J.; Liu, N.; Dorpe, P. V.; Nordlander, P.; Halas, N. J. Plasmonic Transmutation: Introducing New Modes in Nanoclusters by Adding Dielectric Nanoparticles. . *Nano Lett.* **2012**, *12*, 5020-5026.
4. Fan, J. A.; Wu, C.; Bao, K.; Bao, J.; Bardhan, R.; Halas, N. J.; Manoharan, V. N.; Nordlander, P.; Shvets, G.; Capasso, F. Self-Assembled Plasmonic Nanoparticle Clusters. *Science* **2010**, *328*, 1135-1138.
5. Kinkhabwala, A.; Yu, Z.; Fan, S.; Avlasevich, Y.; Müllen, K.; Moerner, W. E. Large single-molecule fluorescence enhancements produced by a bowtie nanoantenna. *Nature Photonics* **2009**, *3*, 654-657.
6. Jain, P. K.; Huang, X. H.; El-Sayed, I. H.; El-Sayed, M. A. Noble Metals on the Nanoscale: Optical and Photothermal Properties and Some Applications in Imaging, Sensing, Biology, and Medicine. *Accounts of Chemical Research* **2008**, *41*, 1578-1586.
7. Sardar, R.; Shumaker-Parry, J. S. Asymmetrically Functionalized Gold Nanoparticles Organized in One-Dimensional Chains. *Nano Letters* **2008**, *8*, 731-736.
8. Brown, L. V.; Sobhani, H.; Lassiter, J. B.; Nordlander, P.; Halas, N. J. Heterodimers: Plasmonic Properties of Mismatched Nanoparticle Pairs. *ACS Nano* **2010**, *4*, 819-832.
9. Sheikholeslami, S.; Jun, Y.-w.; Jain, P. K.; Alivisatos, A. P. Coupling of Optical Resonances in a Compositionally Asymmetric Plasmonic Nanoparticle Dimer. *Nano Lett* **2010**, *10*, 2655-2660.
10. Romo-Herrera, J. M.; Alvarez-Puebla, R. A.; Liz-Marzan, L. M. Controlled assembly of plasmonic colloidal nanoparticle clusters. *Nanoscale* **2011**, *3*, 1304-1315.
11. Fu, A. H.; Micheel, C. M.; Cha, J.; Chang, H.; Yang, H.; Alivisatos, A. P. J. Am. Chem. Soc., 2004, 126, . *Discrete Nanostructures of Quantum Dots/Au with DNA* **2004**, 10832-10833.
12. Oh, E.; Hong, M.-Y.; Lee, D.; Nam, S.-H.; Yoon, H. C.; Kim, H.-S. Inhibition Assay of Biomolecules based on Fluorescence Resonance Energy Transfer (FRET) between Quantum Dots and Gold Nanoparticles. *Journal of the American Chemical Society* **2005**, *127*, 3270-3271.
13. Lin, D.; Wu, H.; Zhang, R.; Pan, W. Enhanced Photocatalysis of Electrospun Ag−ZnO Heterostructured Nanofibers. *Chemistry of Materials* **2009**, *21*, 3479-3484.
14. Liu, N.; Tang, M. L.; Hentschel, M.; Giessen, H.; Alivisatos, A. P. Nanoantenna-enhanced gas sensing in a single tailored nanofocus. *Nat Mater* **2011**, *10*, 631-636.
15. Tan, S. J.; Campolongo, M. J.; Luo, D.; Cheng, W. Building plasmonic nanostructures with DNA. *Nature Nanotech.* **2011**, *6*, 268–276.
16. Pierrat, S.; Zins, I.; Breivogel, A.; Sönnichsen, C. Self-Assembly of Small Gold Colloids with Functionalized Gold Nanorods. *Nano Lett* **2007**, *7*, 259–263.
17. Gschneidtner, T. A.; Fernandez, Y. A. D.; Syrenova, S.; Westerlund, F.; Langhammer, C.; Moth-Poulsen, K. A Versatile Self-Assembly Strategy for the Synthesis of Shape-Selected Colloidal Noble Metal Nanoparticle Heterodimers. *Langmuir* **2014**, *30*, 3041–3050.
18 Liu, K.; Lukach, A.; Sugikawa, K.; Chung, S.; Vickery, J.; Heloise Therien-Aubin; Yang, B.; Rubinstein, M.; Kumacheva, E. Copolymerization of Metal Nanoparticles: A Route to Colloidal Plasmonic Copolymers *Angew. Chem. Int. Ed.* **2014**, *53*, 2648 –2653.
19. Gao, B.; Arya, G.; Tao, A. R. Self-orienting nanocubes for the assembly of plasmonic nanojunctions. *Nat. Nanotech.* **2012**, *7*, 433-437.
20. Gao, B.; Alvi, Y.; Rosen, D.; Lav, M.; Tao, A. R. Designer nanojunctions: orienting shaped nanoparticles within polymer thin-film nanocomposites. *Chem. Comm.* **2013**, *49*, 4382-4384.
21. Turkevich, J.; Stevenson, P. C.; Hillier, J. A study of the nucleation and growth processes in the synthesis of colloidal gold. *Discuss. Faraday Soc.* **1951**, *11*, 55-75.
22. Correa-Duarte, M. A.; Pérez-Juste, J.; Sánchez-Iglesias, A.; Giersig, M.; Liz-Marzán, L. M. Aligning Au Nanorods by Using Carbon Nanotubes as Templates†. *Angew. Chem. Int. Ed.* **2005**, *44*, 4375–4378.
23. Manson, J.; Kumar, D.; Meenan, B. J.; Dixon, D. Polyethylene glycol functionalized gold nanoparticles: the influence of capping density on stability in various media. *Gold Bulletin* **2011**, *44*, 99-105.
24. Hore, M. J. A.; Frischknecht, A. L.; Composto, R. J. Nanorod Assemblies in Polymer Films and Their Dispersion-Dependent Optical Properties. *ACS Macro Lett.* **2012**, *1*, 115–121.
25. Tao, A.; Sinsermsuksakul, P.; Yang, P. Polyhedral Silver Nanocrystals with Distinct Scattering Signatures. *Angewandte Chemie International Edition* **2006**, *45*, 4597-4601.

26. Akcora, P.; Liu, H.; Kumar, S. K.; Moll, J.; Li, Y.; Benicewicz, B. C.; Schadler, L. S.; Acehan, D.; Panagiotopoulos, A. Z.; Pryamitsyn, V.; Ganesan, V.; Ilavsky, J.; Thiyagarajan, P.; Colby, R. H.; Douglas, J. F. Anisotropic self-assembly of spherical polymer-grafted nanoparticles. *Nat. Mater.* **2009**, *8*, 354-359.
27. Hooper, J. B.; Bedrov, D.; Smith, G. D. Supramolecular self-organization in PEO-modified C60 fullerene/water solutions: Influence of polymer molecular weight and nanoparticle concentration. *Langmuir* **2008**, *24*, 4550-4557.

Chapter 4, in full, has been submitted for publication in the CrystEngComm Journal. Gao, Bo, Yahya Alvi, Vincent Li, and Andrea R. Tao. The thesis author was the second investigator of this publication.

5 Preliminary Studies of DNA Mediated Assembly in a Polymer Matrix

5.1 Introduction

DNA nanotechnology has emerged as a possible solution to controllably assemble functional architectures at the nanoscale. The surface of nanoparticles can be modified with complimentary single-stranded DNA, whereby discrete base-pair interactions can be used to coordinate their assembly with other components. Three-dimensional nanoparticle assemblies have been formed through such DNA-mediated interactions.[6] However, these assemblies are typically formed in buffered aqueous environments and structural instability outside of this domain confines its unique organizing potential to a solution-based step which must then be deposited onto a substrate. As was discussed in Chapter 1, DNA directed structures usually have a low particle density and in order to sustain 3-dimensional form the structure must be backfilled with other materials. We believe one possible solution is the use of polymer matrices to potentially stabilize and dictate these DNA directed structures through entropic interactions. If this is possible we want to utilize this to expand DNA assembly to a solid state framework. By addressing DNA stability outside of the aqueous regime, it is possible to break the solution limited application barrier and use this highly precise assembly mechanism to build functional 2-dimensional solid state architectures.

Our assembly plan is laid out in Figure 4.1. Using DNA we wanted to explore two design questions: (1) By depositing a well-dispersed periodic film of particles as a template, could we use DNA assembly to control particle deposition and loading density to create higher order plasmonic architectures using solely bottom up fabrication

techniques? (2) Is DNA miscible in a polystyrene matrix, does it behave like a polymer graft, and can it hybridize to form hierarchical structures with specific coordination and control?

5.2 Experimental

DNA Preparation- Two complimentary thiolated oligonucleotides were purchased from IDT:

DNA1(5'-GCG-CAT-ACT-CGT-CGG-GCG-GCC-TTT-TTT/3thioMC3-D/-3');

DNA2(5'-GGC-CGC-CCG-ACG-AGT-ATG-CGC-TTT-TTT/3thioMC3-D/-3'). The as purchased DNA was used to make a 1 mM stock solution which was kept in the freezer at 4°C. In order to prepare for nanoparticle surface modification, 5 μL of the stock solution was added to 95 μL of 0.1 M Phosphate Buffer ($NaPO_4$, pH = 8). A solution containing 0.1M Dithiothreitol (DTT) was prepared in 0.1 M Phosphate Buffer. 10 μL of the DTT solution was added to the DNA/Buffer solution. After careful mixing, the solution is allowed to incubate for 2 hours at room temperature.

Desalting Column- The existing buffer in the column is rinsed out three times with the addition of deionized water. During the third rinse, 400 μL of deionized water is added to the 110 μL DNA/Buffer/DTT solution. Once the column is almost empty, slowly add the 510 μL DNA solution dropwise into the column. Then elute the solution with 500 μL of deionized water. A total of ~1mL should be collected from the column in this process. This should result in a DNA concentraion fo approximately 5 μM; however, it is necessary to take optical measurements to ensure the proper concentration of the DNA as much can be lost in the column due to adhesion.

DNA Functionalization- DNA solution was added to the particle solution drop-wise. The relative ratio between DNA and particle was always kept constant at 1000:1. The solution was gently mixed every 10 drops and was allowed to incubate for at least ~2 hrs. For surface ligand exchanges, an LB film was first deposited onto a substrate and a droplet of 500 μM DNA was incubated on the surface for ~2 hrs. DNA functionalization was confirmed through both UV-Vis spectroscopy and Zeta potential measurements.

DNA Assembly- For assembly on the polymer interface, a 250 μL droplet of Au particles with their surface modified with the complimentary strand was placed onto the DNA modified Ag cube film. This droplet was allowed to sit for varying times. For assembly in the polymer interface, DNA modified particles were thermally annealed at 65°C into atactic polystyrene (M_w = 1.8k) for varying amounts of time.

4.3 Results and Discussion

5.3.1 DNA mediated assembly at air-polymer interface

After a well dispersed film of Ag nanocubes was functionalized with DNA, we attempted to see whether we could control loading density of Au spheres around the cubes (Figure 4.2). We were able to show that DNA mediated assembly was occuring, however, deposition was uncontrolled. Neither studies varying assembly time with a fixed concentration nor varying concentration of gold spheres added was able to reproducibly show dimer or trimer formation. Figures 4.3c and 4.3d show that gold particles would attach to the side faces of the cubes with random selectivity. The top face was rarely loaded with any particles, we attribute this effect either to excessive washing/drying effects, DNA polymer length allowed for bond flexibility, or that the particles were stabilized by having two interfaces (polystyrene and cube face).

Although the kinetics of the assembly are not well understood at this point, after a long period of time (approx. 3 hours) the cubes would be saturated with a ring of spheres around them (Figure 4.5). At high concentrations of Au spheres and long assembly time, string structures would form interconnecting Ag nanocubes (Figure 4.4). Although, sphere-cube assembly would be preferred through complimentary DNA hybridization, it is possible that sphere-sphere assembly is occurring due to secondary DNA structures forming between similar strands. This assembly result is very exciting because structures similar to these have been reported to have fanoresonant and interesting waveguiding properties.[1,2]

5.3.2 DNA mediated assembly inside polymer matrix

Figure 5.6 shows that DNA coated particles are miscible with a polystyrene matrix. A well dispersed film of DNA modified Ag nanocubes can be annealed into polystyrene matrix as indicated by SEM and the color change of the substrate from a bright green to a darker brown/green color. Assembly results have not been conclusive. Some initial studies of nanocubes with self-similar DNA strands have shown results that may indicate self-similar DNA modified cubes do not assemble very well, if at all (Figure 5.6). However, experiments involving particles with complimentary strands were inconclusive because the particles did not move after long annealing times. This may be due to insufficient thermal annealing that were not able to fully glass the polymer matrix to allow diffusion.

There are many challenges in developing a deposition mechanism that allows for codeposition of two sets of particles (each modified with with own DNA strand which is complimentary to the other). There is also a challenge in matching the glass transition

temperature of the polymer with the melting temperature of the DNA. Because the assembly is dependent on thermally annealing the particles, if the temperature is not ~20°C above the glassing temperature the particles will have difficulty moving, this is an issue because DNA melts near 75°C. This requires a polymer matrix that has a glass transition temperature between 40-50°C, which are very difficult to spincoat with controllable thicknesses.

5.4 Future Outlook

Although the above results are preliminary, they show much promise in the specificity that DNA grafting can provide to the nanoparticle-polymer assembly method. However, there are significant challenges that need to be overcome in both assembly methods. The polymer interface assembly produces hierarchical structures that can potentially exhibit Fano resonances. However, it is necessary to delve further into how the assembly kinetics work so that the role that DNA plays in these assemblies can be understood. In order for assembly inside the polymer matrix, a polymer with a suitable glassing temperature is necessary to continue looking at whether DNA is able to hybridize in the matrix.

Using DNA to dictate solid state architecture will provide a unique framework for building multifunctional devices. By removing the constraints of using DNA in buffered aqueous solutions, DNA nanotechnology can expand as a general technique for nanoscale assembly. It will address the resolution limits in lithography by offering molecular-level precision for nanostructure orientation and placement. Such a method would have significant impact in a broad range of fields where nanostructure assembly is critical,

including the miniaturization of integrated circuits, high resolution sensors, and medical diagnostics.

5.5 Figures

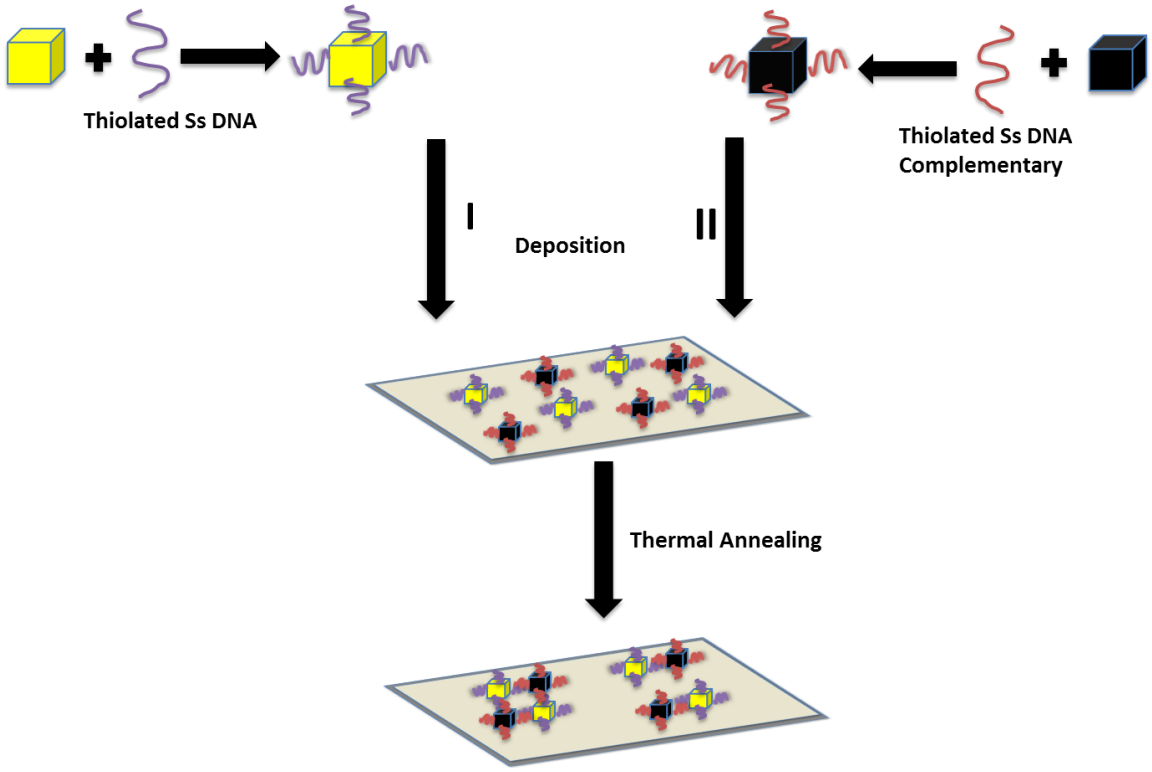

Figure 5.1. DNA mediated assembly inside of a polymer matrix plan. Two sets of particles modified with complimentary oligonucleotides. The particles would be codeposited onto the polystyrene film where they would become imobilized. After thermal anneal the particles would become fully embedded and begin to difuse and interact within the matrix.

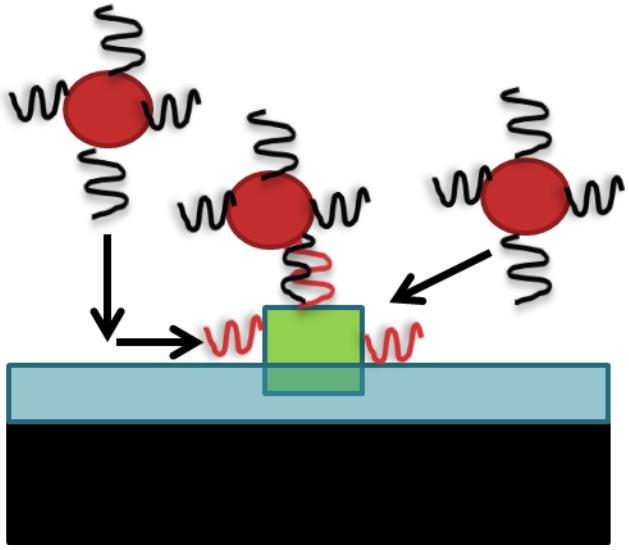

Figure 5.2. Schematic representing air-polymer interface assembly. Ag nanocubes are deposited and imobilized in the polystyrene film. A droplet of particles modified with the complimentary oligonucleotide is placed and assembly occurs.

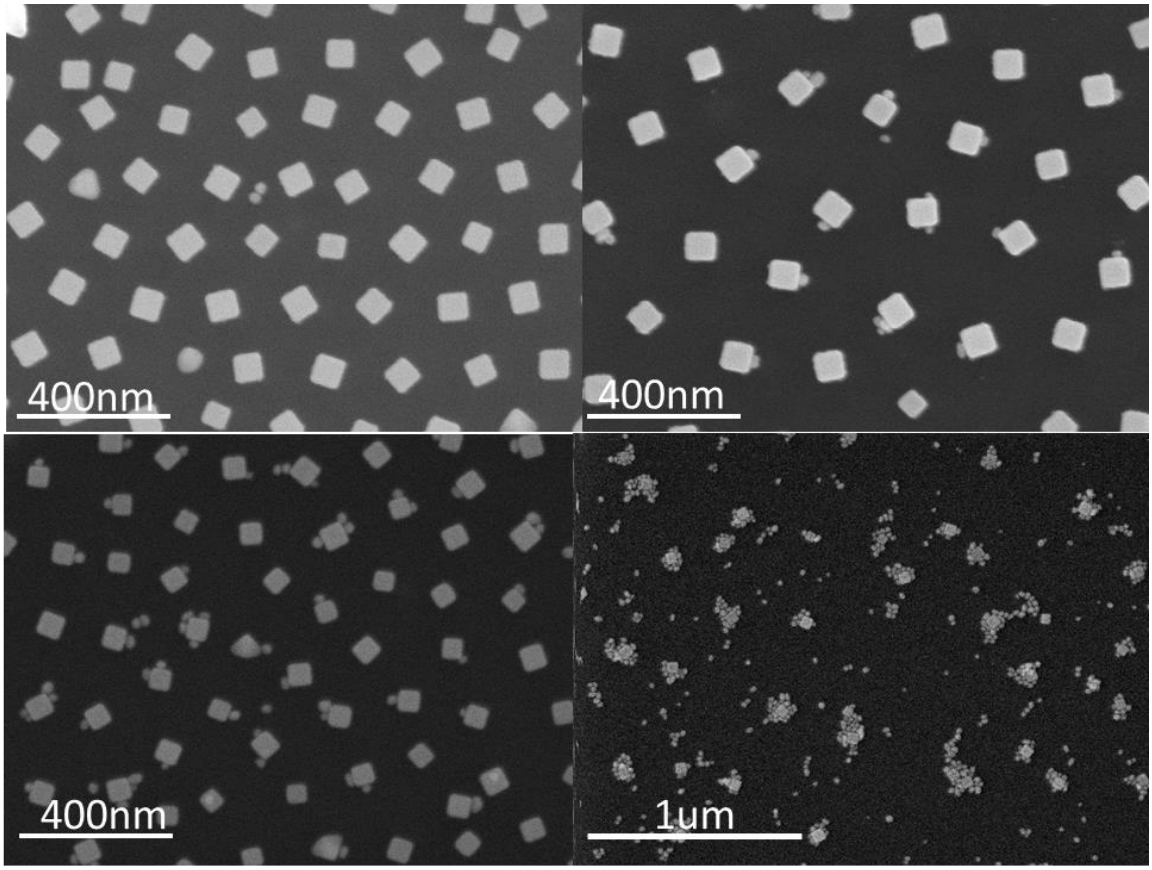

Figure 5.3. SEM images showing air-polymer interface assembly results. (A) After 1hr incubation time, with no DNA modifications present does not result in any attachment. B-C after varying assembly time, attachment is very random and uncontrolled. Every particle has a different number or attachments and this is not consistent through out the films. B: 1 hour. C: 7 hours with a low concentration of gold particles added. D: 7 hours with a high concentration of gold particles added.

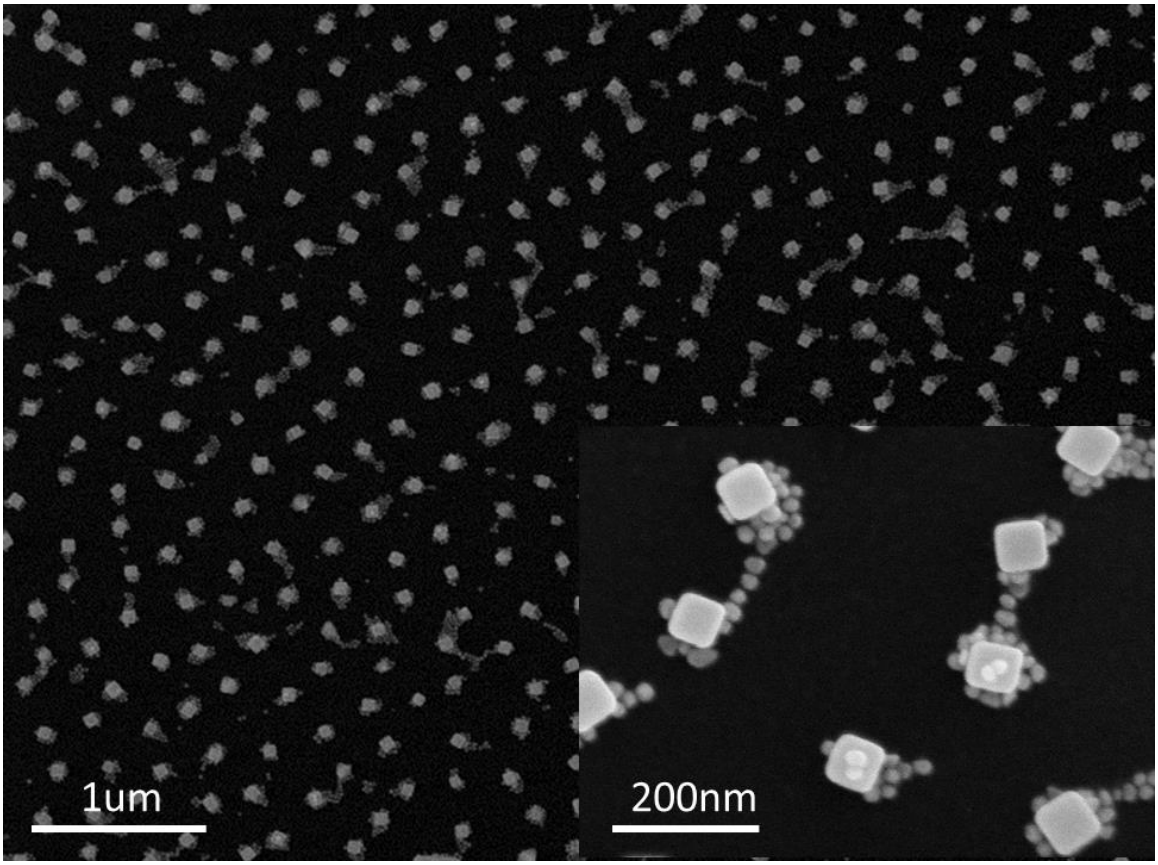

Figure 5.4. SEM image of string structures forming between anchored nanocubes. After 5 hours of assembly time.

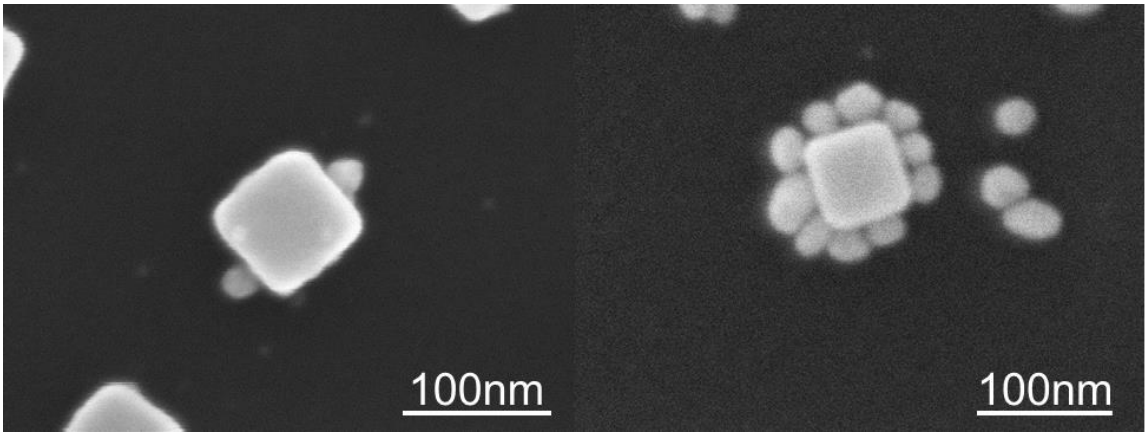

Figure 5.5. Ideal structures that form with this assembly mechanism These ring structures if reproduced may have fanoresonant tendencies.

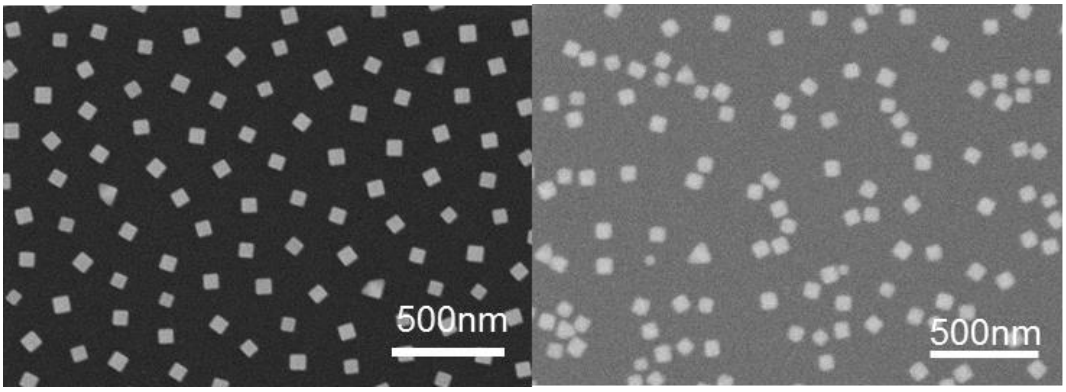

Figure 5.6. The right image shows an initial film of Ag nanocubes modified with the same DNA strands. The left image shows that after 10 hours of thermal annealing at 70°C. There is no specific observable assembly. The particles are moving together but are not orienting.

5.6 References

1. Fan, J. A., Bao, K., Wu, C., Bao, J., Bardhan, R., Halas, N. J., ... & Capasso, F. (2010). Fano-like interference in self-assembled plasmonic quadrumer clusters. *Nano letters*, *10*(11), 4680-4685.
2. Fang, Z., Liu, Z., Wang, Y., Ajayan, P. M., Nordlander, P., & Halas, N. J. (2012). Graphene-antenna sandwich photodetector. *Nano letters*, *12*(7), 3808-3813.
3. Gao, B.; Arya, G.; Tao, A. R. Self-orienting nanocubes for the assembly of plasmonic nanojunctions. *Nat. Nanotech.* **2012**, *7*, 433-437
4. Gao, B.; Arya, G.; Tao, A. R. Self-orienting nanocubes for the assembly of plasmonic nanojunctions. *Nat. Nanotech.* **2012**, *7*, 433-437
5. Gao, B.; Alvi, Y.; Rosen, D.; Lav, M.; Tao, A. R. Designer nanojunctions: orienting shaped nanoparticles within polymer thin-film nanocomposites. *Chem. Comm.* **2013**, *49*, 4382-4384.
6. Mirkin, Chad A., et al. "A DNA-based method for rationally assembling nanoparticles into macroscopic materials." *Nature* 382.6592 (1996): 607-609.
7. Tao, A.; Sinsermsuksakul, P.; Yang, P. Polyhedral Silver Nanocrystals with Distinct Scattering Signatures. *Angewandte Chemie International Edition* **2006**, *45*, 4597-4601.
8. Turkevich, J., Garton, G., & Stevenson, P. C. (1954). The color of colloidal gold.*Journal of colloid Science*, *9*, 26-35.